THE JOURNAL OF COMPARATIVE NEUROLOGY 474:524–534 (2004)

Intrinsic Differences in Brain and Spinal Cord Mitochondria: Implication for Therapeutic Interventions

PATRICK G. SULLIVAN,[1,2] ALEXANDER G. RABCHEVSKY,[1] JEFFERY N. KELLER,[2,3] MARK LOVELL,[3] AJEET SODHI,[4] RONALD P. HART,[4] AND STEPHEN W. SCHEFF[2,3]

[1]Spinal Cord and Brain Injury Research Center, University of Kentucky, Lexington, Kentucky 40536

[2]Department of Anatomy and Neurobiology, University of Kentucky, Lexington, Kentucky 40536

[3]Sanders-Brown Center on Aging, University of Kentucky, Lexington, Kentucky 40536

[4]W.M. Keck Center for Collaborative Neuroscience, Rutgers University, Piscataway, New Jersey 08854

ABSTRACT

It is well known that regions of the CNS differentially respond to insults. After brain injury, cyclosporine A reduces damage but is ineffective following spinal cord injury. We address this disparity by assessing several parameters of mitochondrial physiology in the normal neocortex and spinal cord. In situ measurements of $O_2^{-\cdot}$ production, lipid peroxidation, and mitochondrial DNA oxidation revealed significantly higher levels in spinal cord vs. neocortical neurons. Real-time PCR demonstrated differences in mitochondrial transcripts coupled with decreases in complex I enzyme activity and respiration in spinal cord mitochondria. The threshold for calcium-induced mitochondrial permeability transition was substantially reduced in spinal cord vs. neocortex and modulated by lipid peroxidation. These intrinsic differences may provide a pivotal target for strategies to ameliorate neuronal damage following injury, and this imbalance in oxidative stress may contribute to the susceptibility of spinal cord motor neurons in neuropathologies such as amyotrophic lateral sclerosis. J. Comp. Neurol. 474:524–534, 2004.

Indexing terms: mitochondrial physiology; reactive oxygen species; CNS; motor neurons

Alterations in excitatory amino acids (EAA), increased oxidative stress, and disruption of Ca^{2+} homeostasis are major factors contributing to the ensuing neuropathology in several neuropathologic states, i.e., traumatic brain or spinal cord (SC) injury (TBI or SCI, respectively), recurrent or prolonged seizures, ischemic injury to the brain, amyotrophic lateral sclerosis (ALS), Alzheimer's disease, and Huntington's disease. It is also well documented that, in all these conditions, only certain regions and/or populations of neurons in the CNS succumb to the disease state. We have recently demonstrated differences in therapeutically defined responses between the cortex and the SC following injury (Scheff and Sullivan, 1999; Sullivan et al., 2000b; Rabchevsky et al., 2001a, 2003).

Recent evidence has indicated that mitochondria play a fundamental role in the death cascade (Finkel, 2001; Hunot and Flavell, 2001), and mitochondria have been directly linked to EAA-mediated neurotoxicity (Nicholls and Budd, 1998; Stout et al., 1998; Jiang et al., 2001a; Brustovetsky et al., 2002; Sullivan et al., 2003). These data coupled with evidence that physiological differences exist in mitochondria isolated from different organs (Andreyev et al., 1998; Andreyev and Fiskum, 1999), as well as different regions of the brain (Friberg et al., 1999), raise the possibility that mitochondria localized in the brain and SC may be intrinsically different.

To test this hypothesis, we evaluated in situ reactive oxygen species (ROS) production, levels of lipid peroxidation, and oxidation of mitochondrial DNA (mtDNA) be-

Grant sponsor: National Institutes of Health, U.S. Public Health Service: Grant numbers: NS48191 (P.G.S.) and NS31220 (S.W.S.).

*Correspondence to: Patrick Sullivan, Spinal Cord and Brain Injury Research Center, University of Kentucky, 240 HSRB, Lexington, KY 40536-0305. E-mail: patsull@uky.edu

Received 5 September 2003; Revised 9 December 2003; Accepted 16 February 2004

DOI 10.1002/cne.20130

Published online in Wiley InterScience (www.interscience.wiley.com).

tween normal rat brain and SC tissues. We assayed specific mitochondrial mRNA differences between neocortex and several levels of thoracic SC. Finally, we monitored mitochondrial complex I enzymatic activity, mitochondrial respiration, threshold for Ca^{2+}-induced mitochondrial permeability transition (mPT), and effect of lipid peroxidation on mPT. The results clearly demonstrate that significant differences exist between brain and SC mitochondria in all the parameters measured, helping to explain why certain therapeutic interventions may be beneficial in the brain or the SC, but not both. More important is that understanding the basis for these intrinsic differences in mitochondria may prove pivotal in designing strategies to ameliorate neuronal damage and improve functional outcome following TBI or SCI, as well as shedding light on other neurological disorders in which differences in susceptibility are evident.

MATERIALS AND METHODS

Animals and experimental design

Young adult (250–300 g) male Sprague-Dawley (Harlan Labs) rats (n = 51) were used in these experiments. All animal procedures were approved by the institutional animal care and use committee.

In the first set of experiments, six rats were used to assess ROS production in situ, and an additional three were immunohistochemically examined for DNA oxidative damage in the motor cortex vs. SC. In the second set of experiments, mitochondria were obtained from the neocortex and compared with mitochondria isolated from the thoracic (T) SC (T8–T12). The forebrains and SC tissue of six animals were pooled and used for assessments of mtDNA oxidation, Western blot analysis of 4-hydrononenonal (HNE) expression, and mitochondrial complex I activity. In the third set of experiments, tissue from the same regions of six other animals was again pooled, and the threshold for mPT (mitochondrial swelling), mitochondrial respiration, and mitochondrial mRNA were all assessed. In total three independent sets of experiments were performed for each assay. All the assays for experiments 2 and 3 were run in replicates of three to five per assay and the mean data used for analysis.

In situ measurement of ROS production and DNA oxidative damage

In vivo ROS was measured by using dihydroethidium (DHET; Molecular Probes, Eugene, OR), which is specifically converted to ethidium by $O_2^{-\cdot}$. An i.v. injection of 200 μl DHET (suspended in DMSO at 50 mg/ml and diluted 1:100 with saline for a final concentration of 0.5 mg/ml) was administrated 3 hours before the rats were anesthetized with sodium pentobarbital (95 mg/kg body weight; Nembutal; Abbott Laboratories, North Chicago, IL) and perfused transcardially with physiological saline, followed by phosphate-buffered saline (PBS; pH 7.4) containing 10% formalin (w/v). Brains and spinal cords were removed and postfixed for 24 hours in 10% formalin in PBS and subsequently placed in a solution containing 10% formalin and 20% sucrose for an additional 24 hours. Serial coronal (brain) and longitudinal horizontal (spinal cord) cryosections were cut at 50 μm through the regions of interest and mounted onto gelatin-coated slides. Fluorescence intensity of DHET was assessed microscopically at 500–510 nm excitation and >580 nm emission, and the images were captured with a Spot camera mounted on an Olympus Provis epifluorescent microscope. From four equally spaced sections for each animal, presumptive motor neurons (5–12 per section) in the motor cortex and SC ventral horns were carefully outlined, and the average pixel intensity was calculated for each animal with Image-Pro Plus (version 4.5.1).

To examine DNA oxidative damage in the motor cortex vs. the SC ventral horns, anesthetized rats were perfused with 4% paraformaldehyde in PBS. The brain and SC (T8–T12) were immediately dissected and postfixed for 1 hour at 4°C before cryoprotecting them in 20% sucrose/PBS at 4°C overnight. Serial coronal (brain) or longitudinal (SC) cryosections were cut at 40 μm through the regions of interest and mounted onto gelatin-coated slides. Air-dried tissue sections were incubated overnight at room temperature in PBS containing 0.3% Triton X-100, 3% normal horse serum (Vector, Burlingame, CA), and a monoclonal antibody against 8-hydroxyguanosine (oh^{8}G)-bovine serum albumin (BSA) and -casein conjugates (5 μg/ml; QED Bioscience Inc.), which is a specific marker of oxidative damage to DNA and RNA. After several washes in PBS, biotinylated horse anti-mouse (1:200; Vector) diluted in PBS with 0.3% Triton X-100 was applied overnight at room temperature. The ABC method was then employed by using streptavidin-fluorescein isothiocyanate (FITC; 1:300; Vector) as the fluorochrome. Control slides had the primary antibody omitted. Additionally, to ensure specificity of staining, adjacent slides were incubated with 40 μg/ml RNase or DNase (Sigma, St. Louis, MO) in the blocking buffer for 1 hour at 37°C prior to overnight incubation at room temperature with the primary antibody. When all rinses were complete, the sections were mounted with Vectashield (Vector). Presumptive motoneurons in the motor cortex and SC ventral horn were examined for immunoreactivity against oxidative damage to DNA and/or RNA in each animal. The fluorescence images were captured by using both a Magnafire camera mounted onto an Olympus BX-51 epifluorescent microscope and a Leica TCS laser scanning confocal system with an argon light for FITC with a Leica DM RXE microscope.

Mitochondrial preparation

Nonsynaptosomal mitochondria were prepared as previously described, with slight medications (Sullivan et al., 2000a, 2003). The animals were anesthetized with an overdose of sodium pentobarbital (95 mg/kg body weight; Nembutal; Abbott Laboratories) and transcardically perfused with 30 ml ice-cold homogenization buffer (250 mM sucrose, 20 mM HEPES, 0.1% BSA, 1 mM EGTA, pH 7.2). The animals were then decapitated and the brains carefully dissected and minced with scissors in 10 ml ice-cold homogenization buffer. The SC was extruded from the spinal column by inserting an 18-g needle connected to a syringe full of homogenization buffer into the lumbar thecal sac and forcefully squirting out the entire spinal cord through the rostral foramen caused by decapitation. A 2-cm segment (T8–T12) was excised and minced with scissors in 10 ml ice-cold homogenization buffer. All subsequent steps were conducted at 4°C. The tissue was rinsed with 10 ml homogenization buffer and processed (eight strokes) with a hand-held tissue homogenizer (Thomas Scientific). The resulting homogenate was centrifuged for 10 minutes at 1,300*g*. The supernatant was

collected and again centrifuged at 10,000*g* for 10 minutes. The pellet was gently resuspended (four or five strokes) in 5 ml of homogenization buffer with a hand-held homogenizer, placed atop a discontinuous Ficoll gradient (7.5%, 10%), and centrifuged at 100,000*g* for 30 minutes as previously described (Lai and Clark, 1979; Sullivan et al., 2000a, 2003). The final pellet was resuspended in EGTA-free homogenization buffer and washed by centrifugation (14,500*g* and 7,500*g* for 10 minutes), yielding purified nonsynaptosomal mitochondria. The final pellet was stored on ice at a concentration of 10 mg/ml. Mitochondrial protein concentration was determined by using a Pierce BCA kit (Pierce, Rockfrod, IL).

Western blot analysis of mitochondrial HNE, mitochondrial DNA oxidation, and complex I activity and respiration and mitochondrial swelling

Mitochondrial lipid peroxidation was assessed by performing Western blots with an antibody directed against HNE as previously described (Keller et al., 2000). Aliquots (150–300 μg) of mitochondrial protein were taken, a protease inhibitor cocktail (Sigma) was added, and the sample was frozen in liquid nitrogen and stored at –70°C. Mitochondrial protein concentration was determined with a Pierce BCA kit, and exactly 5 μg of solubilized mitochondrial protein was loaded per lane and separated by electrophoresis in a 12% polyacrylamide gel, transferred to a nitrocellulose sheet, and immunoreacted with primary antibody (anti-HNE monoclonal antibody; 1:2,500; Chemicon, Temecula, CA). The nitrocellulose was then further processed by using anti-mouse secondary antibody (1:2,000) and an ECL Western blotting kit according to the manufacturer's protocol (Amersham Pharmacia Biotech, Piscataway, NJ); then, the films were scanned and the densitometric measurements quantified by outlining the reactive bands first in the SC lanes, then overlaying the same bands/areas in the cortex lanes to obtain average pixel intensities with NIH Image software (Sullivan et al., 2002).

Quantification of total mtDNA oxidation was measured by using gas chromatography/mass spectrometry as previously described (Gabbita et al., 1998). mtDNA was isolated as follows: sodium dodecyl sulfate (SDS) was added to a 1-mg aliquot of isolated mitochondria, for a concentration of 1%, and incubated at 37°C for 1 hour to promote complete lysis. A 1/4 volume of saturated NaCl (55°C) was added and the mixture cooled to 4°C. The SDS and protein precipitate was removed by centrifugation at 10,000*g* for 5 minutes, and the supernatant purified by using freshly prepared phenol, phenol/chloroform, and chloroform with phase-lock gel tubes. The mtDNA was precipitated overnight in 2 volumes of 100% ETOH at –20°C and resuspended in 400 μl TE. The mtDNA was then treated with 100 μg/ml RNAase for 1 hour at 37°C, then precipitated with Na-acetate as described above. Quantification of total mtDNA oxidation was measured by using gas chromatography/mass spectrometry as previously described (Gabbita et al., 1998). Stable, isotope-labeled, oxidized base analogues were used as internal standards to measure nucleotide base oxidation, which was expressed as nanomoles per microgram mtDNA.

Complex I activity was measured in isolated mitochondria as the rotenone-sensitive decrease in NADH absorption at 340 nm with ubiquinone-1 as the final acceptor, as previously described (Sriram et al., 1998), with slight modifications. Briefly, mitochondria were freeze-thawed and sonicated three times. The assay was performed in 25 mM KPO_4 buffer (pH 7.2) containing mitochondrial protein (100–150 μg), 5 mM $MgCl_2$, 1 mM KCN, 1 mg/ml BSA, and 150 μM NADH. The reaction was preincubated for 2 minutes at 30°C, the baseline established, and the reaction initiated by addition of coenzyme Q-1 (50 μM). The loss of absorbance at 340 nm was monitored over time. The assay was also performed in the presence of rotenone (10 μM) to determine the rotenone-insensitive activity and the rotenone-sensitive complex I enzyme activity calculated by subtracting the rotenone-insensitive activity from the total activity. We additionally adapted the protocol for a 96-well plate and measured complex I activity by monitoring NADH fluorescence (340 nm excitation, >450 nm emission) over time under the same conditions as described above.

Mitochondrial oxygen consumption was measured by using a Clark-type electrode in a continuously stirred, sealed chamber (Oxygraph System; Hansatech Instruments Ltd.) at 37°C as previously described (Sullivan et al., 2000a, 2003; Jiang et al., 2001b; Sensi et al., 2003). Isolated mitochondrial protein (100–500 μg) was suspended in respiration buffer (250 mM sucrose, 20 mM HEPES, 2 mM $MgCl_2$, 2.5 mM inorganic phosphates, 0.1% BSA, pH 7.2) in a final volume of 0.5 ml. Respiratory control ratio (RCR) was calculated as the ratio of oxygen consumption in the presence of 5 mM glutamate and 2.5 mM malate or 10 mM succinate before (state 4) and after (state 3) the addition of ADP.

Mitochondria undergo a catastrophic swelling after the opening of the mitochondrial permeability transition pore (mPTP). A direct measure of this swelling is the decrease in absorbance (light scattering) of isolated mitochondria in suspension. Accordingly, the mPT was assessed as previously described (Sullivan et al., 1999b, 2000a; Jiang et al., 2001a; Sensi et al., 2003). Briefly, 100–250 μg of isolated cortical and SC mitochondrial protein were suspended in 1 ml of respiration buffer plus 10 mM succinate. After a 5-minute preincubation at 37°C and baseline measurements, $CaCl_2$ was added to the cuvette to yield a final concentration of 20, 50, or 100 nmol/mg of mitochondrial protein. The MPT (mitochondrial swelling) was measured as a decrease in absorbance (540 nm) by using a spectrophotometer over 2–10 minutes following the addition of $CaCl_2$. Maximal swelling was induced by incubation of mitochondria with 30 mM HEPES-buffered KCl, and, for data analysis, Ca-independent changes in absorbance were subtracted, and mitochondria swelling was expressed as the loss of absorbance per unit time per microgram of mitochondrial protein (arbitrary units). Additions of cyclosporin A (CsA; Sigma), 5 μM bongkrekic acid (Biomol Research Labs), and 1–100 μM HNE (Caymen Chemical Co.) were made during the preincubation, and these substances were present throughout the experiment.

Real-time PCR

Rat neocortex or SC was dissected, frozen on powdered dry ice, and stored at –70°C. The SC was divided into five sections, each 5 mm long, centered on T9/10. Tissues were homogenized in Trizol (Invitrogen, La Jolla, CA) and chloroform extracted, and the aqueous phase was made to 35%

TABLE 1. Gene-Specific Primer Pairs Used for RT-PCR

Gene	Accession No.	Sequence
ATP SYN/ATPsynthase subunit C	NM_017311	Forward 5′-GGAACCCGTCTCTCAAGCAG-3′ Reverse 5′-CAAAGCCCAGGATGGCATAG-3′
Cyclophilin D	U68544	Forward 5′-GTGAGAAGGGCTTTGGCTACA-3′ Reverse 5′-CTGGGATGACCCTGTGGAAG-3′
ND2/NADH dehydrogenase subunit 2	NC_001665	Forward 5′-AACTTGGACTAGCCCCATTCC-3′ Reverse 5′-TTCCTTGGGTGACTTCGGG-3′
ND3/NADH dehydrogenase subunit 3	NC_001665	Forward 5′-ACCCATATGAATGTGGCTTCG-3′ Reverse 5′-AAAAAGGAAGGCGTGCAGAA-3′
COX II/cytochrome b oxidase II	NC_001665	Forward 5′-TTTGAACAATTCTCCCAGCTGTC-3′ Reverse 5′-GGGAGGGAAGGGCAATTAGA-3′
ND4/NADH dehydrogenase subunit 4	NC_001665	Forward 5′-TGATTATCACAACCCAACGAGG-3′ Reverse 5′-GGAGGTTGTTTATGTGGCTGGT-3′
ND4L/NADH dehydrogenase subunit 4L	NC_001665	Forward 5′-CCATAATCTCCATAACCATCCCA-3′ Reverse 5′-CGCAGGCTGCAAAAACTAGAAT-3′
GAPDH/glyceraldehyde dehydrogenase	NM_017008.1	Forward 5′-AACTCCCTCAAGATTGTCAGCAA-3′ Reverse 5′-GGCTAAGCAGTTGGTGGTGC-3′

with ethanol, then loaded onto an RNeasy column (Qiagen, Chatsworth, CA). The column was washed and RNA eluted following the manufacturer's recommendations. Specific mitochondrial or nuclear mRNA levels were obtained by quantitative reverse transcription-PCR (RT-PCR) with selected gene-specific primer pairs (Table 1). RNA was reverse transcribed with SuperScript II (Invitrogen) and random primers as suggested by the manufacturer. The PCRs were carried out by using 10 ng of cDNA, 50 nM of each primer, and SYBR green master mix (Applied Biosystems, Foster City, CA) in 10-μl reactions. Quantities of PCR product were measured by using SYBR green fluorescence (Ririe et al., 1997; Wittwer et al., 1997) collected during real-time PCR on an Applied Biosystems 7900HT system. A control cDNA dilution series was created for each gene to establish a standard curve. Each reaction was subjected to melting-point analysis to confirm single amplified products.

Statistical considerations

For all analyses, the significance of differences among groups was set at $P < .05$. Data were evaluated with Student's t-test and corrected for multiple measurements by using the Benjamini and Hochberg false discovery rate at $P < .05$ when required.

Photomicrograph production

The photomicrographs in Figures 1 and 3 were assembled and converted to black and white in Adobe Photoshop 7.0. Only the contrast and brightness of the photomicrographs were adjusted.

RESULTS

Significant differences exist in basal levels of ROS production in SC and cortical neurons

In situ ROS production was measured with DHET, which is specifically converted to ethidium by $O_2^{-\cdot}$. Microscopic examination revealed conspicuous qualitative differences in ethidium fluorescence in presumptive cortical motor neurons compared with SC motor neurons from the same animal (Fig. 1a). This difference was apparent in all animals examined, indicating that the basal levels of ROS production were markedly increased in SC motor neurons. Semiquantitative analysis confirmed that the difference in ethidium fluorescence was significant, with the average optical density increased by 140% in individual SC motor neurons compared with presumptive cortical motor neurons (Fig. 1b).

Mitochondrial lipid peroxidation and DNA oxidation are significantly increased in the SC compared with cortex: significance decreases in complex I activity

The increase ROS production indicated by DHET conversion in the SC could be due to differences in uptake of the indicator between brain and SC; however, this indicator is very specific for $O_2^{-\cdot}$, by virtue of acting as a scavenger in a terminal reaction with $O_2^{-\cdot}$ to form the fluorescent product ethidium. If, indeed, in situ $O_2^{-\cdot}$ production is increased in the SC, it should be evident by measuring downstream markers of increased oxidative stress, including lipid peroxidation and mtDNA oxidation. Insofar as mitochondria are the primary sites of ROS production in cells, they are also a prominent target for such oxidative damage.

To address these questions, nonsynaptic mitochondria were isolated from the forebrain and SC of rats, and oxidative damage was assessed in mitochondrial proteins and mtDNA. Western blot analysis of mitochondrial proteins revealed a significant increase in the levels of the highly toxic lipid peroxidation byproduct HNE (Fig. 2a,b) in the SC compared with the cortex. Qualitatively, it appeared that mitochondria isolated from the spinal cord had much higher HNE content, as evident from several bands reactive to HNE (Fig. 2), which would be expected, given the nonspecific cross-linking of proteins by HNE in vivo. It was also apparent that several bands reactive in the SC were not reactive in the cortical mitochondria. Optical density measurements of the bands verified that HNE levels in SC mitochondria were significantly elevated (40%) compared with cortical mitochondria.

Increased levels of ROS production and oxidative stress would also be expected to lead to DNA damage. This scenario may be especially important for mtDNA because of its proximity to the source of the ROS production and the lack of histones protecting mtDNA from oxidative damage. As expected, the levels of oxidized bases in mtDNA were significantly higher in SC mitochondria compared with cortical mitochondria (Fig. 3a), confirming that SC ROS production and subsequent oxidative are increased compared with the cortex.

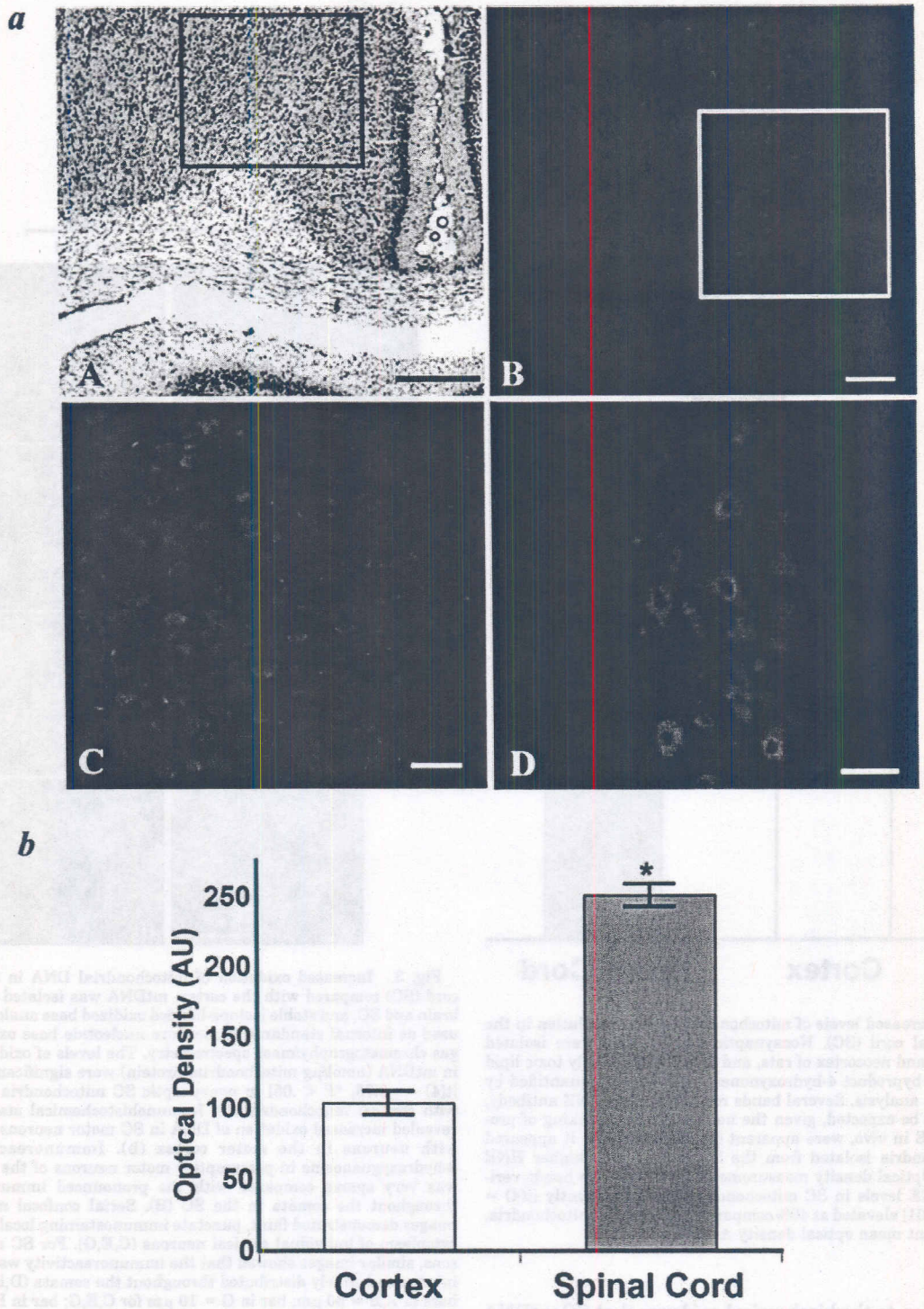

Fig. 1. Neurons in the spinal cord (SC) produce higher levels of reactive oxygen species (ROS) compared with cortical neurons. In situ ROS production measured in the cortex and SC by using dihydroethidium (DHET), which is specifically converted to fluorescent ethidium by $O_2^{-\cdot}$ (**a**). The converted DHET was then quantified at the cellular level by measuring fluorescence intensity (**b**). a: The boxed area in A demarcates the rat motor cortex (M2, M1; Paxinos and Watson, 1998), stained with cresyl violet, which is represented in B showing basal levels of ethidium fluorescence. Note the relatively higher levels of ROS in presumptive cortical motor neurons (boxed area in B) compared with adjacent regions. Microscopic comparison of ethidium fluorescence in presumptive cortical motor neurons (C; higher magnification of boxed area in B) vs. spinal cord ventral horn motor neurons (D) showed markedly increased basal levels of ROS production in the spinal cords of all animals examined. Quantitative analysis (b) revealed that the difference in ROS levels was significant [$t(4) = -12.48$, $^*P < .001$], with a 140% increase in the optical density (AU) of ethidium fluorescence in randomly sampled SC motor neurons compared with presumptive cortical motor neurons. Scale bars = 0.5 mm in A, 100 μm in B, 50 μm in C,D.

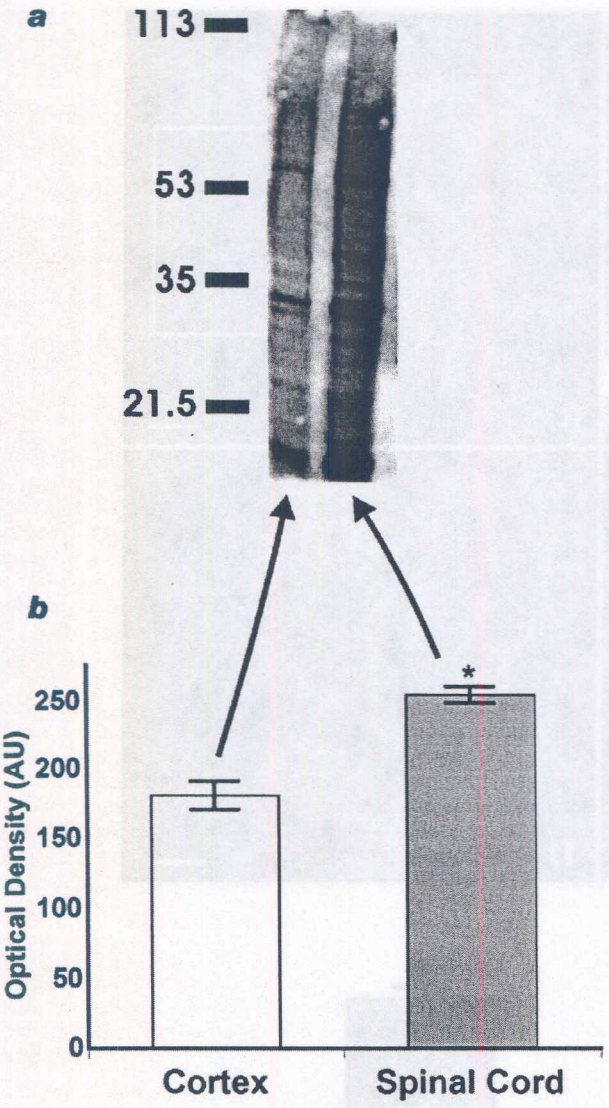

Fig. 2. Increased levels of mitochondrial lipid peroxidation in the normal spinal cord (SC). Nonsynaptic mitochondria were isolated from the SC and neocortex of rats, and levels of the highly toxic lipid peroxidation byproduct 4-hydroxynonenal (HNE) were quantified by Western blot analysis. Several bands reactive for the HNE antibody, which would be expected, given the nonspecific cross-linking of proteins by HNE in vivo, were apparent (**a**). Qualitatively, it appeared that mitochondria isolated from the SC had a much higher HNE content. **b:** Optical density measurements of the various bands verified that HNE levels in SC mitochondria were significantly [$t(4) = -6.16$, $^*P < .01$] elevated at 40% compared with cortical mitochondria. Bars represent mean optical density ± SEM.

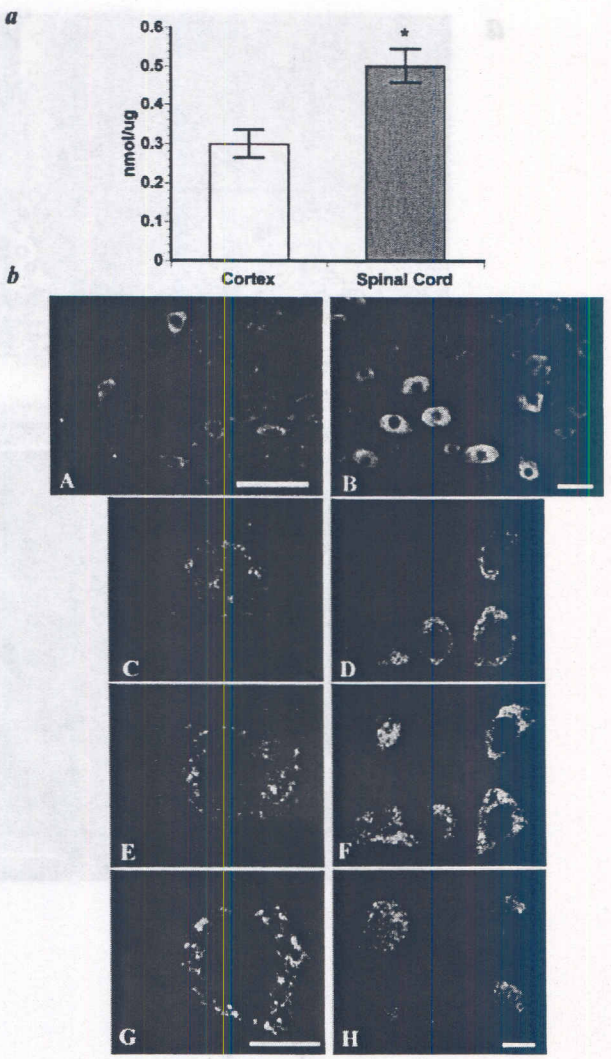

Fig. 3. Increased oxidation of mitochondrial DNA in the spinal cord (SC) compared with the cortex. mtDNA was isolated from forebrain and SC, and stable isotope-labeled oxidized base analogues were used as internal standards to measure nucleotide base oxidation by gas chromatography/mass spectrometry. The levels of oxidized bases in mtDNA (nmol/μg mitochondrial protein) were significantly higher [$t(4) = -3.75$, $^*P < .05$] in nonsynaptic SC mitochondria compared with cortical mitochondria (**a**). Immunohistochemical staining also revealed increased oxidation of DNA in SC motor neurons compared with neurons in the motor cortex (**b**). Immunoreactivity for 8-hydroxyguanosine in presumptive motor neurons of the cortex (A) was very sparse compared with the pronounced immunolabeling throughout the somata in the SC (B). Serial confocal microscopic images demonstrated faint, punctate immunostaining localized to the cytoplasm of individual cortical neurons (C,E,G). For SC motor neurons, similar images showed that the immunoreactivity was far more intense and widely distributed throughout the somata (D,F,H). Scale bars in A,B = 50 μm; bar in G = 10 μm for C,E,G; bar in H = 10 μm for D,F,H.

In addition to the biochemical evidence that SC mtDNA oxidation is increased, immunohistochemical staining revealed increased oxidation of DNA in the SC compared with the cortex (Fig. 3b). Immunoreactivity for 8-hydroxyguanosine in presumptive motor neurons of the cortex was very sparse compared with the pronounced immunolabeling in the SC (Fig. 3bA,B). Confocal microscopy revealed faint punctate immunostaining localized to the cytoplasm of individual cortical motor neurons (Fig. 3bC,E,G). In contrast, in the somata of SC motor neurons,

the immunoreactivity was far more intense and widely distributed (Fig. 3bD,F,H). The cytoplasmic staining preferentially reflected oxidized DNA, insofar as it was not affected by RNase pretreatment but was eliminated by DNase pretreatment of the tissue sections (not shown).

The mitochondrial genome encodes 13 peptides, seven of which are complex I subunits. The significant increase in mtDNA oxidization in the SC that we measured could affect the transcription of mitochondrial encoded genes in the SC and affect normal mitochondrial function. Additionally, complex I is the most complex member of the ETS, with over 40 subunits, making it a prime candidate for increased lipid peroxidation damage and loss of function. Complex I activity was measured as the rotenone-sensitive decrease in NADH absorption in mitochondria isolated from forebrain and SC. A significant reduction in complex I enzyme activity was measured in nonsynaptic SC mitochondria compared with forebrain mitochondria (Fig. 4a). The complex I activities (nmol of NADH oxidized/min/mg of protein) that we measured are similar to those previously reported by Sriram and colleagues (1998). However, those authors did not make direct comparisons between brain and SC regions but, instead, mad comparisons within the same regions of brain and SC before and after drug treatment.

This reduction in enzyme activity translated into a significant loss of NADH substrate-linked (complex I driven) respiration (Fig. 4b). We assessed NADH substrate-linked (pyruvate and malate as substrates) respiration (complex I-driven respiration) and measured significant reductions in SC mitochondria oxygen consumption compared with cortical mitochondria in states II, III, IV, and V (Fig. 4b). No significant differences were measured when succinate (complex II-driven respiration) was used as the substrate, with the exception of state V respiration [$t(4) = 3.69$, $P < .05$].

Relative levels of mitochondrial mRNAs in neocortex and SC

To determine whether differences in mitochondrial function were associated with differences in gene expression, we assayed several mitochondrial mRNAs by using real-time PCR (Fig. 5). SC samples were sectioned into five 5-mm tissue samples, because spinal cord varies over its length with respect to the proportion of white matter and relative neuronal content (Rabchevsky et al., 2001b, 2002).

Several mitochondrial mRNAs were found to be reduced in SC. Most prominently, NADH dehydrogenase subunit 3 (ND3) was significantly lower in all regions of SC tested than in neocortex. Several mRNAs, including NADH dehydrogenase subunits 2 (ND2) and 4 (ND4) were reduced in T7 but not in more distal samples. Cytochrome c oxidase (COX II) was reduced only in T7 and T12 segments, and cyclophilin D mRNA was significantly increased in levels T11 of the SC compared with neocortex (1.58-fold, $P = .014$). By comparison, the postsynaptic density protein PSD95, which we predicted would be proportionally increased in brain because of a higher concentration of synapses, was reduced in all segments of SC. Each RNA measured was expressed as a ratio to GAPDH mRNA to correct for variations in input cDNA, and direct measurements of GAPDH mRNA showed no differences between cortex and SC (not shown). These results indicate that the intrinsic differences in mitochondrial metabolism exist

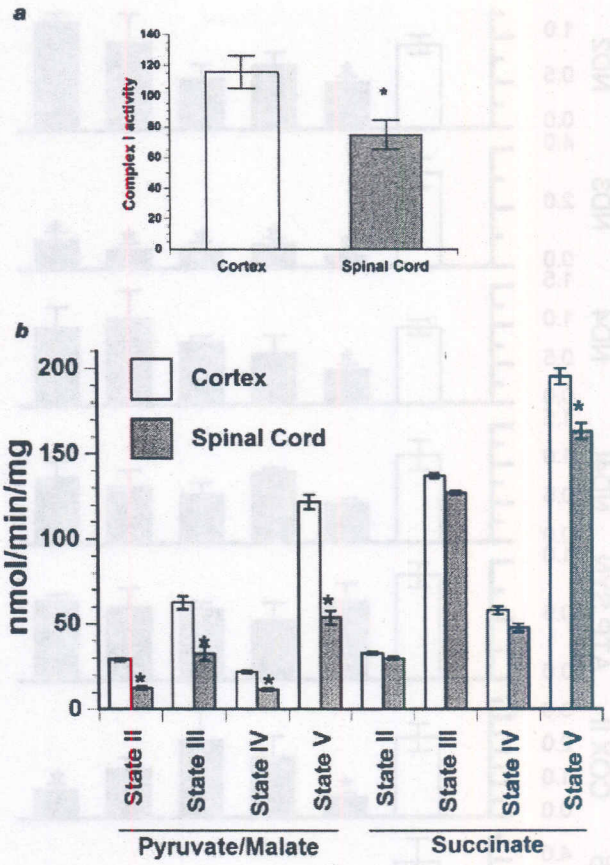

Fig. 4. Decreased complex I activity and function in the normal spinal cord (SC). Complex I enzyme activity was measured as the rotenone-sensitive decrease in NADH absorption in sonicated mitochondria isolated from forebrain and SC. A significant [$t(4) = 2.82$, $*P < .05$] reduction in complex I enzyme activity (y-axis; nmol NADH oxidized/min/mg protein) was measured in nonsynaptic SC mitochondria compared with forebrain mitochondria (**a**). In intact mitochondria, NADH substrate-linked respiration (complex I-driven respiration) was significantly [$t(4) = 6.92$, $*P < .01$] reduced in SC mitochondria compared with cortical mitochondria in states II, III, IV, and V (**b**). No significant differences were measured when succinate (complex II-driven respiration) was used as the substrate, with the exception of state IV respiration [$t(4) = 3.69$, $*P < .05$].

even at the genomic level and could possibly stem from increased oxidative stress in SC neurons.

Differences in the threshold for permeability transition in cortical and SC mitochondria: modulation of the threshold by HNE

The mPT has been implicated in several different paradigms of neurodegeneration shown to be directly modulated by ROS production. We assessed the threshold for mPT in rat cortex and SC, in light of our findings demonstrating increased ROS production and oxidative damage in SC mitochondria. Representative traces are shown in Figure 6 and illustrate that the addition of 20 nmol Ca^{2+}/mg mitochondrial protein induced a rapid swelling

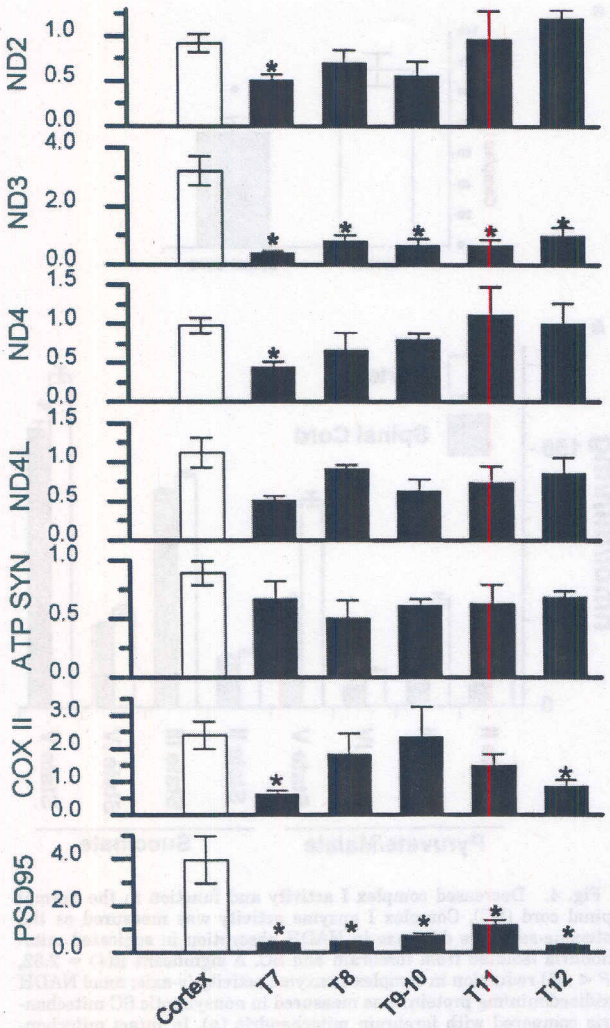

Fig. 5. Reduced mitochondrial gene expression in the normal spinal cord (SC). Total cellular RNA was prepared from neocortex and several 5-mm segments of thoracic SC, reverse transcribed, and assayed by SYBR green fluorescence on real-time PCR. Results are shown as ratios of each mRNA concentration to GAPDH mRNA in arbitrary units. Bars represent mean ± SEM (n = 4). An asterisk denotes significant difference from cortex by Student's *t*-test, corrected for multiple measurements using the Benjamini and Hochberg false discovery rate at $*P < .05$.

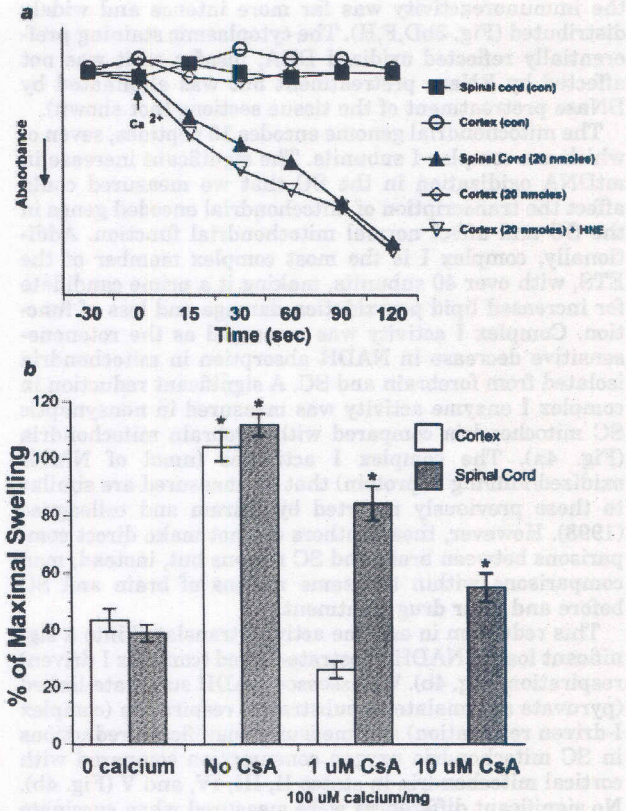

Fig. 6. Differences in the threshold for permeability transition in cortical and spinal cord (SC) mitochondria. Nonsynaptic mitochondria were isolated from the neocortex and SC of rats, and the induction of mPT was monitored by following light absorbance decreases, indicative of mitochondrial swelling (a). The addition of 20 nmol Ca^{2+}/mg of mitochondrial protein induced a rapid loss of absorbance in SC mitochondria but had little effect on cortical mitochondria. Preincubation of cortical mitochondria with the lipid peroxidation product HNE (10 μM) reduced the threshold for Ca^{2+}-induced mPT to the same level demonstrated in SC mitochondria. Concentrations of Ca^{2+} greater than 100 nmol/mg (100 μM) induced CsA-sensitive swelling in both cortical and SC mitochondria (b). Mitochondrial swelling was expressed as a percentage of swelling measured in cortical or SC mitochondria suspended in hypoosmotic buffer. Preincubation of cortical mitochondria with 1 μM CsA completely inhibited Ca^{2+}-induced swelling but had little effect on SC mitochondria. Increasing the concentration of CsA to 10 μM further reduced Ca^{2+}-induced swelling in SC mitochondria but did completely inhibit the loss of absorbance. $*P < .05$ compared with 0 Ca^{2+}; bars represent group mean ± SEM.

in SC mitochondria but had little effect on cortical mitochondria. Ca^{2+} concentrations in excess of 80 nmol/mg of mitochondria protein induced classic mPT in both the SC and the cortical mitochondria (Fig. 6b), which was effectively blocked by the addition of 5 μM bongkrekic acid (cortex 15% ± 2.4%, SC 18% ± 3.6% of maximum swelling). CsA was also partially effective; however, much higher concentrations than previously reported were needed (Fig. 6b) in the SC.

Preincubation of cortical mitochondria with 10 μM HNE reduced the threshold for Ca^{2+}-induced mPT to the same level demonstrated in SC mitochondria (Fig. 6). Concentrations of HNE ranging from 1 to 100 μM also significantly reduced the mPT threshold in a dose-dependent manner (data not shown). Pretreatment of the mitochondria with 1 mM of the reducing agent dithiothreitol (12% ± 4.4% of maximal swelling), the antioxidant glutathione monoethyl ester (8% ± 3.8% of maximal swelling), or 1 μM CsA (14% ± 6.3% of maximal swelling) inhibited the effect of HNE on cortical mitochondria. The effect of HNE was not mimicked when using 50 μM of other nonneurotoxic lipid peroxidation byproducts (i.e., nonenal, malondialdehyde, trans-2-nonenal; respectively, 2.5% ± 0.9%, 1.8% ± 0.6%, 3.6% ± 0.7% of maximal swelling).

DISCUSSION

Our results clearly demonstrate that several biochemical parameters used to measure mitochondrial function and integrity are significantly divergent in tissue isolated from normal brain and SC of rodents. Differences were measured with respect to in situ ROS production, mitochondrial lipid peroxidation, mtDNA oxidation, and complex I enzyme activity as well as NADH-linked respiration. Furthermore, specific mitochondrial mRNA levels were reduced in segments of SC compared with cortex. Finally, differences existed in the threshold for Ca^{2+}-induced mPT. Taken together these intrinsic differences between brain and SC mitochondria provide a plausible explanation for the differential effects of certain therapeutic interventions following TBI and SCI.

Several pathophysiological events following CNS trauma are believed to contribute to neuronal damage and death, including glutamate-mediated excitotoxicity, formation of ROS, and subsequent lipid peroxidation (Faden et al., 1989; Braughler and Hall, 1992; Azbill et al., 1997; Sullivan et al., 1998, 1999b). Free radical production is a byproduct of ATP generation in mitochondria as electrons leak from the electron transport system. ROS generation has been shown to increase after glutamate exposure (Coyle and Puttfarcken, 1993; Dugan et al., 1995) and has been directly linked to Ca^{2+} influx into the mitochondria (Reynolds and Hastings, 1995; Prehn, 1998; Scanlon and Reynolds, 1998; Sengpiel et al., 1998; Carriedo et al., 2000; Liang et al., 2000). Furthermore, ROS production and lipid peroxidation increase following experimental TBI (Sullivan et al., 1998) or SCI (Braughler and Hall, 1992; Hall et al., 1992; Azbill et al., 1997) and in ALS (Andrus et al., 1998; Hall et al., 1998), and reduction of ROS production at the level of the mitochondria has been shown to be neuroprotective in several paradigms (Keller et al., 1998; Sullivan et al., 1999a; Liang et al., 2000). An imbalance between ROS production and its removal has also been proposed for neurological diseases, including ALS, which leads to a progressive degeneration of SC motor neurons, particularly as it relates to mitochondrial function (Beal, 1995; Bowling and Beal, 1995).

Our present data demonstrate a significant increase in the in situ basal production of $O_2^{-\cdot}$ in motor neurons of the SC compared with cortical motor neurons. Normally, cells are able to convert mitochondrial $O_2^{-\cdot}$ to H_2O_2, utilizing both mitochondrial manganese superoxide dismutase and cytosolic copper-zinc superoxide dismutase. Given the high reactivity and small diffusion radius of ROS, one would predict that unsaturated fatty acids in membranes and macromolecules (mtDNA) closest to the source of ROS production would be especially vulnerable to damage. In support of this, we measured significantly higher levels of HNE in mitochondria isolated from the SC compared with brain. Additionally, we found significantly higher levels of oxidized mtDNA in the SC compared with the brain, both at the biochemical and at the immunohistochemical levels, reflecting localization of mtDNA to the primary source of ROS production. Along with other possibilities, this increase in oxidized mtDNA may have resulted in altered mitochondrial genomic transcription, as evidenced by decreased levels of several mitochondrial mRNAs in the SC.

Most of the mitochondrial mRNAs we examined were reduced in at least one region of SC compared with cortex. The most striking difference was found in ND3, which exhibited reduced mRNA levels in all segments of thoracic SC tested. Several other subunits of NADH dehydrogenase (complex I) were also reduced in selected cord segments, each consistent with reduced complex I activity and respiration. Complex I is very sensitive to thiol oxidation, and direct inactivation can occur by oxidation (Sriram et al., 1998; Bautista et al., 2000). The complex I activities we measured are similar to those previously reported by Sriram and colleagues (1998). However, those authors did not make direct comparisons between the brain and SC regions but, instead, made comparisons within the same regions of brain and SC before and after drug treatment, as noted above. We also observed reduced complex IV (cytochrome c oxidase) mRNA levels, which would explain the reduction in complex II-driven maximal respiration that we measured.

Our results demonstrate that SC mitochondria have a reduced threshold for Ca^{2+}-induced mPT. The induction of the mPT was effectively blocked by using bongkrekic acid, a modulator of the adenine nucleotide translocator, which is a main component of the mPT pore (Halestrap and Davidson, 1990; Halestrap et al., 1997). Additionally, we were able to block the mPT with the established inhibitor CsA; however, for the SC, we had to use concentrations that were much higher than those needed to inhibit mPT in cortical mitochondria, and the inhibition was only partial. It has been reported that CsA and its ability to block mPT are modulated by several factors, including substrate limitation, free fatty acids, Ca^{2+} load, membrane potential, and oxidative stress (Brustovetsky and Dubinsky, 2000).

The addition of HNE to cortical mitochondria lowered their threshold for mPT to that seen in SC mitochondria. This effect was specific for HNE and could be effectively blocked by reducing agents or antioxidants. These data imply that the reduced threshold for mPT in SC mitochondria could be, in part, due to the increased levels of HNE present in the SC and may help to explain our findings of reduced inhibition of the mPT with CsA in the SC (Rabchevsky et al., 2001a). CsA inhibits pore opening by binding to matrix cyclophilin D and blocking its binding to the adenine nucleotide translocator. We also found increased cyclophilin D mRNA levels in T11 SC compared with cortex, which could also decrease the effectiveness of CsA.

Recent reports from our laboratory and others have demonstrated that therapeutic intervention with CsA following experimental TBI is remarkably neuroprotective (Okonkwo et al., 1999; Okonkwo and Povlishock, 1999; Scheff and Sullivan, 1999; Sullivan et al., 1999b, 2000a,b). At least part of the mechanism by which CsA affords neuroprotection is via the maintenance of mitochondrial homeostasis by inhibiting the opening of the MPTP (Buki et al., 1999; Okonkwo et al., 1999; Okonkwo and Povlishock, 1999; Scheff and Sullivan, 1999; Sullivan et al., 1999b). However, when CsA is administered following experimental SCI at the same dosage and regimen used in our TBI paradigms, it has no beneficial effects on histological sparing (Rabchevsky et al., 2001a). This differential response to CsA treatment may be in part due to the compromised bioenergetic integrity of SC mitochondria, leading to a constant state of increased oxidative stress, decreased ATP production capacity, and increased sensitivity to disruptions in Ca^{2+} homeostasis.

In conclusion, the present study clearly demonstrates that significant intrinsic differences exist between mito-

chondria isolated from the normal brain vs. SC. This may partially explain our previous studies demonstrating that certain therapeutic interventions are efficacious after TBI or SCI, but not both. Of further importance are the implications of these findings for other neurodegenerative diseases, particularly ALS, for which ROS and mitochondrial dysfunction in SC motor neurons have been hypothesized to play a pivotal role (Beal, 1995; Bowling and Beal, 1995). Our findings suggest a plausible reason for why mutations in copper-zinc superoxide dismutase seen in familial ALS patients and transgenic mice (Rosen et al., 1993; Gurney et al., 1994) affects predominantly only SC motor neurons. It is clear that future studies are needed to elucidate completely the extent and nature of these physiological differences as well as the underlying mechanisms responsible for such divergence in mitochondria from different regions of the CNS. Once these intrinsic differences are understood, however, their functional ramifications will be instrumental in designing successful pharmacological strategies to minimize tissue damage following TBI and SCI as well as in other neuropathologies that stem from mitochondrial dysfunction.

ACKNOWLEDGMENTS

R.P.H. was supported by the New Jersey Commission on Spinal Cord Research and the Spinal Cord Injury Project of the W.M. Keck Center for Collaborative Neuroscience of Rutgers University.

LITERATURE CITED

Andreyev A, Fiskum G. 1999. Calcium induced release of mitochondrial cytochrome c by different mechanisms selective for brain vs. liver. Cell Death Differ 6:825–832.

Andreyev AY, Fahy B, Fiskum G. 1998. Cytochrome c release from brain mitochondria is independent of the mitochondrial permeability transition. FEBS Lett 439:373–376.

Andrus PK, Fleck TJ, Gurney ME, Hall ED. 1998. Protein oxidative damage in a transgenic mouse model of familial amyotrophic lateral sclerosis. J Neurochem 71:2041–2048.

Azbill RD, Mu X, Bruce-Keller AJ, Mattson MP, Springer JE. 1997. Impaired mitochondrial function, oxidative stress and altered antioxidant enzyme activities following traumatic spinal cord injury. Brain Res 765:283–290.

Bautista J, Corpas R, Ramos R, Cremades O, Gutierrez JF, Alegre S. 2000. Brain mitochondrial complex I inactivation by oxidative modification. Biochem Biophys Res Commun 275:890–894.

Beal MF. 1995. Aging, energy, and oxidative stress in neurodegenerative diseases. Ann Neurol 38:357–366.

Bowling AC, Beal MF. 1995. Bioenergetic and oxidative stress in neurodegenerative diseases. Life Sci 56:1151–1171.

Braughler JM, Hall ED. 1992. Involvement of lipid peroxidation in CNS injury. J Neurotrauma 9(Suppl 1):S1–S7.

Brustovetsky N, Dubinsky JM. 2000. Limitations of cyclosporin A inhibition of the permeability transition in CNS mitochondria. J Neurosci 20:8229–8237.

Brustovetsky N, Brustovetsky T, Jemmerson R, Dubinsky JM. 2002. Calcium-induced cytochrome c release from CNS mitochondria is associated with the permeability transition and rupture of the outer membrane. J Neurochem 80:207–218.

Buki A, Okonkwo DO, Povlishock JT. 1999. Postinjury cyclosporin A administration limits axonal damage and disconnection in traumatic brain injury. J Neurotrauma 16:511–521.

Carriedo SG, Sensi SL, Yin HZ, Weiss JH. 2000. AMPA exposures induce mitochondrial $Ca^{(2+)}$ overload and ROS generation in spinal motor neurons in vitro. J Neurosci 20:240–250.

Coyle JT, Puttfarcken P. 1993. Oxidative stress, glutamate, and neuronal degenerative disorders. Science 262:689–695.

Dugan LL, Sensi SL, Canzoniero LM, Handran SD, Rothman SM, Lin TS, Goldberg MP, Choi DW. 1995. Mitochondrial production of reactive oxygen species in cortical neurons following exposure to N-methyl-D-aspartate. J Neurosci 15:6377–6388.

Faden AI, Demediuk P, Panter SS, Vink R. 1989. The role of excitatory amino acids and NMDA receptors in traumatic brain injury. Science 244:798–800.

Finkel E. 2001. The mitochondrion: is it central to apoptosis? Science 292:624–626.

Friberg H, Connern C, Halestrap AP, Wieloch T. 1999. Differences in the activation of the mitochondrial permeability transition among brain regions in the rat correlate with selective vulnerability. J Neurochem 72:2488–2497.

Gabbita SP, Lovell MA, Markesbery WR. 1998. Increased nuclear DNA oxidation in the brain in Alzheimer's disease. J Neurochem 71:2034–2040.

Gurney ME, Pu H, Chiu AY, Dal Canto MC, Polchow CY, Alexander DD, Caliendo J, Hentati A, Kwon YW, Deng HX, et al. 1994. Motor neuron degeneration in mice that express a human Cu,Zn superoxide dismutase mutation. Science 264:1772–1775.

Halestrap AP, Davidson AM. 1990. Inhibition of Ca2(+)-induced large-amplitude swelling of liver and heart mitochondria by cyclosporin is probably caused by the inhibitor binding to mitochondrial-matrix peptidyl-prolyl cis-trans isomerase and preventing it interacting with the adenine nucleotide translocase. Biochem J 268:153–160.

Halestrap AP, Woodfield KY, Connern CP. 1997. Oxidative stress, thiol reagents, and membrane potential modulate the mitochondrial permeability transition by affecting nucleotide binding to the adenine nucleotide translocase. J Biol Chem 272:3346–3354.

Hall ED, Braughler JM, McCall JM. 1992. Antioxidant effects in brain and spinal cord injury. J Neurotrauma 9(Suppl 1):S165–S172.

Hall ED, Andrus PK, Oostveen JA, Fleck TJ, Gurney ME. 1998. Relationship of oxygen radical-induced lipid peroxidative damage to disease onset and progression in a transgenic model of familial ALS. J Neurosci Res 53:66–77.

Hunot S, Flavell RA. 2001. Apoptosis: death of a monopoly? Science 292: 865–866.

Jiang D, Sullivan PG, Sensi SL, Steward O, Weiss JH. 2001a. Zn^{2+} induces permeability transition pore opening and release of pro-apoptotic peptides from neuronal mitochondria. J Biol Chem 276:47524–47529.

Jiang D, Sullivan PG, Sensi SL, Steward O, Weiss JH. 2001b. $Zn^{(2+)}$ induces permeability transition pore opening and release of pro-apoptotic peptides from neuronal mitochondria. J Biol Chem 276: 47524–47529.

Keller JN, Kindy MS, Holtsberg FW, St Clair DK, Yen HC, Germeyer A, Steiner SM, Bruce-Keller AJ, Hutchins JB, Mattson MP. 1998. Mitochondrial manganese superoxide dismutase prevents neural apoptosis and reduces ischemic brain injury: suppression of peroxynitrite production, lipid peroxidation, and mitochondrial dysfunction. J Neurosci 18:687–697.

Keller JN, Huang FF, Zhu H, Yu J, Ho YS, Kindy TS. 2000. Oxidative stress-associated impairment of proteasome activity during ischemia-reperfusion injury. J Cereb Blood Flow Metab 20:1467–1473.

Lai JC, Clark JB. 1979. Preparation of synaptic and nonsynaptic mitochondria from mammalian brain. Methods Enzymol 55:51–60.

Liang LP, Ho YS, Patel M. 2000. Mitochondrial superoxide production in kainate-induced hippocampal damage. Neuroscience 101:563–570.

Nicholls DG, Budd SL. 1998. Mitochondria and neuronal glutamate excitotoxicity. Biochim Biophys Acta 1366:97–112.

Okonkwo DO, Povlishock JT. 1999. An intrathecal bolus of cyclosporin A before injury preserves mitochondrial integrity and attenuates axonal disruption in traumatic brain injury. J Cereb Blood Flow Metab 19: 443–451.

Okonkwo DO, Buki A, Siman R, Povlishock JT. 1999. Cyclosporin A limits calcium-induced axonal damage following traumatic brain injury. Neuroreport 10:353–358.

Paxinos G, Watson C. 1998. The rat brain in stereotaxic coordinates. San Diego: Academic Press.

Prehn JH. 1998. Mitochondrial transmembrane potential and free radical production in excitotoxic neurodegeneration. Naunyn Schmiedebergs Arch Pharmacol 357:316–322.

Rabchevsky AG, Fugaccia I, Sullivan PG, Scheff SW. 2001a. Cyclosporin A treatment following spinal cord injury to the rat: behavioral effects and stereological assessment of tissue sparing. J Neurotrauma 18:513–522.

Rabchevsky AG, Fugaccia I, Sullivan PG, Scheff SW. 2001b. Cyclosporin A

treatment following spinal cord injury to the rat: behavioral effects and stereological assessment of tissue sparing. J Neurotrauma 18:513–522.

Rabchevsky AG, Fugaccia I, Sullivan PG, Blades DA, Scheff SW. 2002. Efficacy of methylprednisolone therapy for the injured rat spinal cord. J Neurosci Res 68:7–18.

Rabchevsky AG, Sullivan PG, Fugaccia I, Scheff SW. 2003. Creatine diet supplement for spinal cord injury: influences on functional recovery and tissue sparing in rats. J Neurotrauma 20:659–669.

Reynolds IJ, Hastings TG. 1995. Glutamate induces the production of reactive oxygen species in cultured forebrain neurons following NMDA receptor activation. J Neurosci 15:3318–3327.

Ririe KM, Rasmussen RP, Wittwer CT. 1997. Product differentiation by analysis of DNA melting curves during the polymerase chain reaction. Anal Biochem 245:154–160.

Rosen DR, Siddique T, Patterson D, Figlewicz DA, Sapp P, Hentati A, Donaldson D, Goto J, O'Regan JP, Deng HX, Rahmmani Z, Krizus A, McKenna-Yasek D, Cayabyab A, Gaston SM, Berger R, Tanzi RE, Halperin JJ, Herzfeldt B, Van den Bergh R, Hung WY, Bird T, Deng G, Mulder DW, Smyth C, Laing NG, Soriano E, Pericak-Vance MA, Haines J, Rouleau GA, Gusella JS, Horvitz HR, Brown RH. 1993. Mutations in Cu/Zn superoxide dismutase gene are associated with familial amyotrophic lateral sclerosis. Nature 362:59–62.

Scanlon JM, Reynolds IJ. 1998. Effects of oxidants and glutamate receptor activation on mitochondrial membrane potential in rat forebrain neurons. J Neurochem 71:2392–2400.

Scheff SW, Sullivan PG. 1999. Cyclosporin A significantly ameliorates cortical damage following experimental traumatic brain injury in rodents. J Neurotrauma 16:783–792.

Sengpiel B, Preis E, Krieglstein J, Prehn JH. 1998. NMDA-induced superoxide production and neurotoxicity in cultured rat hippocampal neurons: role of mitochondria. Eur J Neurosci 10:1903–1910.

Sensi SL, Ton-That D, Sullivan PG, Jonas EA, Gee KR, Kaczmarek LK, Weiss JH. 2003. Modulation of mitochondrial function by endogenous Zn^{2+} pools. Proc Natl Acad Sci USA 100:6157–6162.

Sriram K, Shankar SK, Boyd MR, Ravindranath V. 1998. Thiol oxidation and loss of mitochondrial complex I precede excitatory amino acid-mediated neurodegeneration. J Neurosci 18:10287–10296.

Stout AK, Raphael HM, Kabterewucz BI, Klann E, Reynolds IJ. 1998. Glutamate-induced neuron death requires mitochondrial calcium uptake. Nat Neursci 1:366–373.

Sullivan PG, Keller JN, Mattson MP, Scheff SW. 1998. Traumatic brain injury alters synaptic homeostasis: implications for impaired mitochondrial and transport function. J Neurotrauma 15:789–798.

Sullivan PG, Bruce-Keller AJ, Rabchevsky AG, Christakos S, Clair DK, Mattson MP, Scheff SW. 1999a. Exacerbation of damage and altered NF-kappaB activation in mice lacking tumor necrosis factor receptors after traumatic brain injury. J Neurosci 19:6248–6256.

Sullivan PG, Thompson MB, Scheff SW. 1999b. Cyclosporin A attenuates acute mitochondrial dysfunction following traumatic brain injury. Exp Neurol 160:226–234.

Sullivan PG, Geiger JD, Mattson MP, Scheff SW. 2000a. Dietary supplement creatine protects against traumatic brain injury. Ann Neurol 48:723–729.

Sullivan PG, Rabchevsky AG, Hicks RR, Gibson TR, Fletcher-Turner A, Scheff SW. 2000b. Dose-response curve and optimal dosing regimen of cyclosporin A after traumatic brain injury in rats. Neuroscience 101: 289–295.

Sullivan PG, Keller JN, Bussen WL, Scheff SW. 2002. Cytochrome c release and caspase activation after traumatic brain injury. Brain Res 949:88–96.

Sullivan PG, Dube C, Dorenbos KD, Steward O, Baram TZ. 2003. Mitochondrial uncoupling protein-2 protects the immature brain from excitotoxic neuronal death. Ann Neurol 53:711–717.

Wittwer CT, Ririe KM, Andrew RV, David DA, Gundry RA, Balis UJ. 1997. The LightCycler: a microvolume multisample fluorimeter with rapid temperature control. Biotechniques 22:176–181.